

## REVIEW

# Advanced magnetic resonance imaging biomarkers of cerebral metastases

S.J. Mills<sup>a</sup>, G. Thompson<sup>b</sup>, A. Jackson<sup>a,b</sup>

<sup>a</sup>Department of Neuroradiology, Salford Royal Foundation Trust Hospital, Salford, Greater Manchester, UK;

<sup>b</sup>Wolfson Molecular Imaging Centre, 27 Palatine Road, University of Manchester, Manchester, M20 3LJ, UK

Corresponding address: S. Mills, Department of Neuroradiology, Salford Royal Foundation Trust Hospital, Salford, Greater Manchester, UK. Email: samantha.mills@srft.nhs.uk

Date accepted for publication 27 January 2012

### Abstract

There are a number of magnetic resonance imaging techniques available for use in the diagnosis and management of patients with cerebral metastases. This article reviews these techniques, in particular, the advanced imaging methodologies from which quantitative parameters can be derived, the role of these imaging biomarkers have in distinguishing metastases from primary central nervous system tumours and tumour mimics, and metrics that may be of value in predicting the origin of the primary tumour.

**Keywords:** Cerebral metastases; MRI; Biomarkers; Perfusion; Diffusion; Spectroscopy.

### Introduction

This article reviews the magnetic resonance imaging (MRI) techniques available for use in the diagnosis and management of patients with cerebral metastases. Particular attention is paid to advanced imaging methodologies from which quantitative parameters can be derived, the role of these imaging biomarkers in distinguishing metastases from primary central nervous system (CNS) tumours and tumour mimics, and metrics that may be of value in predicting the origin of the primary tumour.

Cerebral metastases are believed to account for up to 50% of brain tumours. This is likely to be a significant underestimation<sup>[1]</sup>. Autopsy studies have reported an incidence of cerebral metastases of up to 25% in patients with systemic cancer<sup>[2,3]</sup>. With advancements in the management of patients with systemic malignancy, there has been a decline in patients dying from uncontrolled systemic disease. Cancer patients are surviving longer and whilst their systemic disease is controlled with newer medications, an increase in CNS dissemination has been reported<sup>[1,4,5]</sup>.

Cerebral metastases are a leading cause of mortality in patients with metastatic malignancy and the median survival for those patients receiving whole brain

radiotherapy (WBRT) is 7 months<sup>[6]</sup>. Surgical resection of solitary metastases has been shown to convey a survival advantage in patients with systemically controlled disease in a small number of studies, but this is diminished in the presence of small, additional, non-resectable metastases<sup>[7]</sup>. In addition, stereotactic radiosurgery (SRS) is increasingly being utilized in the treatment of multiple (up to 4) small (less than 3 cm maximum diameter) metastases, although the advantages of this technique over WBRT for the treatment of more than 2 lesions remains controversial<sup>[8,9]</sup>. It is therefore imperative that imaging provides accurate diagnosis, identification, size information and localization of all intracranial lesions in patients with presumed cerebral metastatic disease in order to optimize their management.

### Diagnosis

The differential diagnosis of the solitary enhancing cerebral mass, of which metastatic disease is one of the leading causes, can be a major diagnostic challenge in neuroradiology. Approximately 50% of cerebral metastases are solitary. Whilst multiplicity favours the diagnosis of metastatic disease, differentiation from multifocal glioblastoma multiforme (GBM) and tumour mimics such as

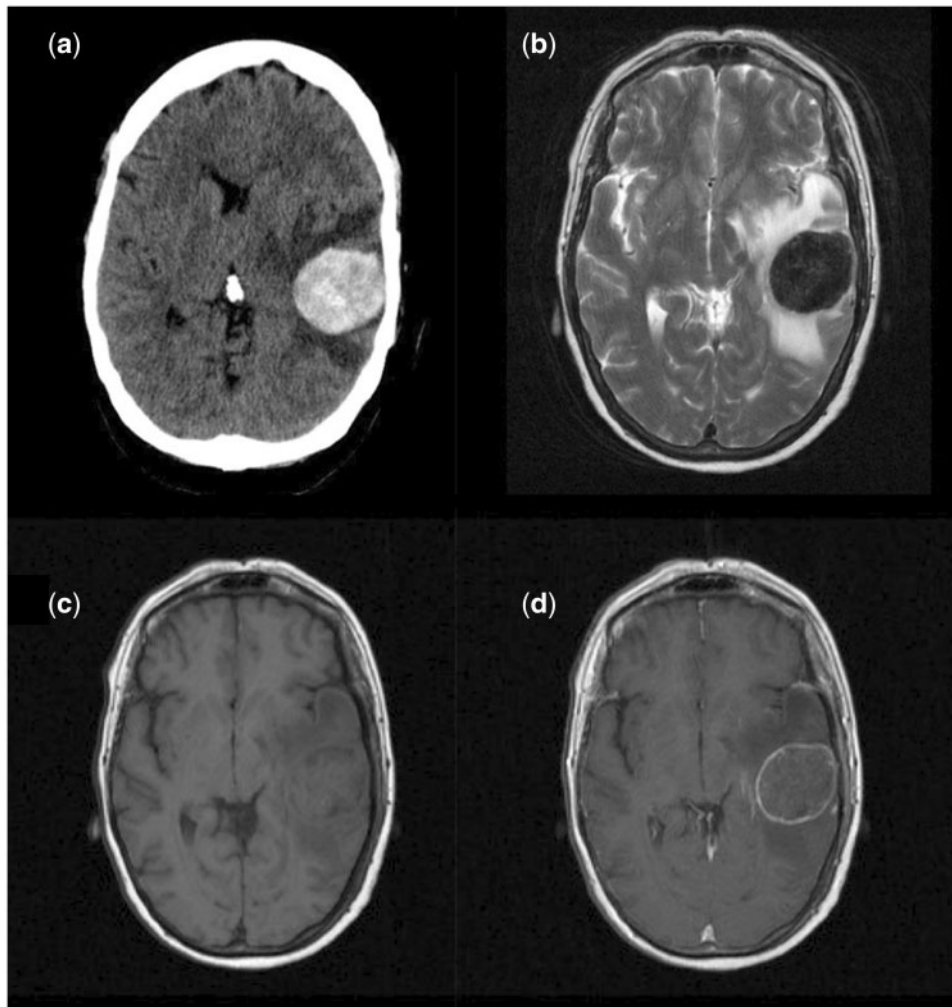


**Figure 1** Imaging appearances of a solitary mucinous metastases from a colonic carcinoma primary on (a) non-contrast CT (hyper-attenuating lesion); (b)  $T_2$ -weighted imaging (markedly hypointense); (c)  $T_1$ -weighted pre-contrast imaging (isointense); (d) post-gadolinium contrast  $T_1$ -weighted imaging (rim enhancement).

infection or tumefactive demyelination can be difficult. Distinction between these entities and metastatic disease is important with regard to both immediate patient management, and the need for additional imaging in patients with no known malignancy to identify a primary site and treat appropriately.

### Conventional imaging

Classically, cerebral metastases are seen on either computed tomography (CT) scanning or MRI as lesions occurring at the cortical interface at the grey and white matter junction, most commonly located within the cerebral hemispheres followed by the cerebellum. Lesions can vary from radiologically silent microscopic deposits to masses measuring several centimetres in diameter. Contrast enhancement is frequently seen and can be intense, punctate, nodular or ring enhancing. Haemorrhage can also be a feature, and occurs more frequently in certain underlying primary pathologies

(see below). The degree of peri-tumoural oedema varies from virtually none to (more commonly) extensive surrounding oedema. MRI exhibits superior sensitivity to CT for small lesion identification, particularly in the posterior fossa, and double/triple dose contrast, delayed imaging and the use of magnetization transfer to suppress background signal from non-enhancing tissues can further improve the sensitivity of lesion detection<sup>[10,11]</sup>. In addition, certain imaging characteristics such as high attenuation on non-contrast CT and low T2 signal intensity as seen in mucinous metastases (Fig. 1) or high signal on non-contrast T1 imaging of melanoma metastases (Fig. 2), can suggest the underlying primary lesion. The utilization of alternative conventional sequences such as contrast-enhanced multi-shot echo planar fluid attenuated inversion recovery (FLAIR)<sup>[12]</sup> and pre- and post-contrast inversion recovery T1-weighted sequences<sup>[13]</sup> instead of conventional T1 spin echo sequences have failed to demonstrate benefit in improving lesion conspicuity. Phenotypic descriptors such as

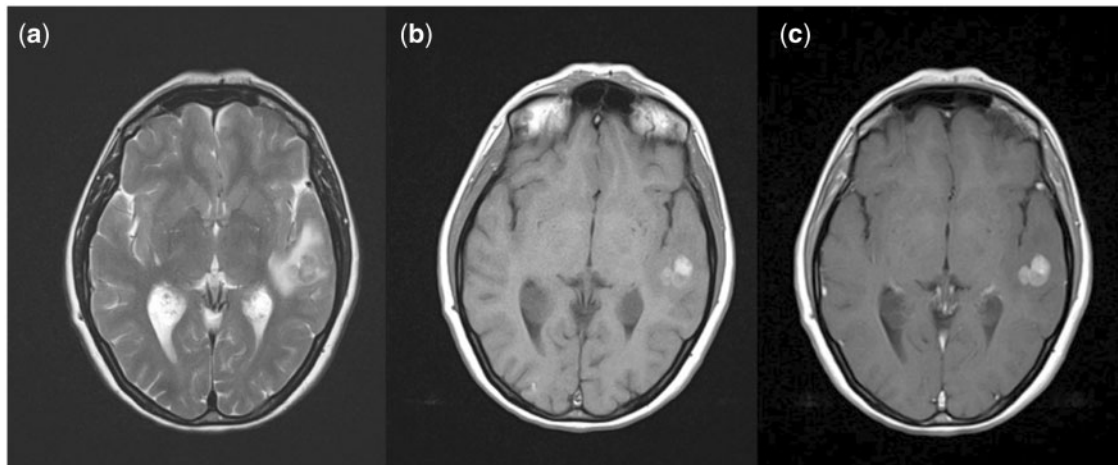


**Figure 2** Imaging characteristics of melanoma metastases. (a) T<sub>2</sub>; (b) pre-contrast T<sub>1</sub>; (c) post-contrast T<sub>1</sub>.

non-enhancing cortical FLAIR signal abnormality adjacent to the mass lesion have been described more frequently in glioma but this feature is also seen in some cases of cerebral metastases<sup>[14]</sup>.

The relative volume of signal hyperintensity on FLAIR or T<sub>2</sub>-weighted imaging to the enhancing lesion volume is frequently cited as a good discriminator of malignant glioma and cerebral metastases in radiology textbooks. A greater degree of peri-lesional signal change, commonly referred to as oedema although the underlying content in glioma is more complex, is reportedly indicative of metastatic disease rather than glioma. The published literature supporting this is scant, however. A small ( $n = 29$ ) CT-based study from 1989 reported differences in the mean ratio of oedema volume to tumour volume between metastases (3.1) and primary lesions (1.4)<sup>[15]</sup>. A more recent MRI study of 26 metastases and 22 high-grade gliomas (HGG) evaluated the peritumoural oedema to tumour area ratio, and found significant differences between HGG ( $0.69 \pm 0.41$ ) and metastases ( $2.41 \pm 1.63$ ),  $P < 0.001$ <sup>[16]</sup>. More evidence actually supports the use of advanced imaging metrics in the peri-lesional oedema to discriminate these 2 entities as detailed below, reflecting the underlying pathological differences in the origin of this signal change.

### Perfusion/permeability imaging

Dynamic contrast-enhanced (DCE) imaging techniques have been developed that allow for a number of parameters to be estimated that are thought to reflect the microvascular environment. Detailed descriptions of these methodologies are beyond the scope of this review and interested readers are directed to a number of excellent review articles on the subject of perfusion and permeability imaging in neuro-oncology<sup>[17–20]</sup>. In brief, a bolus of contrast agent is injected intravenously and tracked with a series of dynamic images. Baseline

longitudinal relaxivity (T<sub>1</sub>) is measured, and changes in T<sub>1</sub>-weighted signal intensity are converted to changes in contrast agent concentration. Contrast agent concentration time courses are generated, and post-processing of the data with application of pharmacokinetic modelling techniques allows for the calculation of a number of parameters, the most widely used of which is  $K^{\text{trans}}$  (contrast volume transfer coefficient, in effect the amount of contrast passing from the intravascular space to the extravascular, extracellular space) reflecting both local blood flow and capillary permeability. For dynamic susceptibility contrast techniques (DSC-MRI), the contrast agent bolus is tracked using fast T<sub>2</sub>- or T<sub>2</sub>\*-weighted acquisitions. Models of differing complexity can be used but the fundamental goal is to derive estimates of cerebral blood volume (CBV) and cerebral blood flow (CBF).

In distinguishing primary from metastatic cerebral tumours, the only parameter reported to have value in robustly separating the 2 entities is CBV. A number of studies have reported higher CBV values in the solid tumour component of HGGs than in metastases<sup>[21–30]</sup>. Furthermore, in the examination of the peri-tumoural so-called oedematous region (peri-lesional T<sub>2</sub>/FLAIR signal hyperintensity seen adjacent to enhancing or clearly solid tumour mass), HGGs are reported to demonstrate higher CBV values than metastases<sup>[30–33]</sup> (Fig. 3). This may reflect differences in the underlying mechanisms of the so-called peri-tumoural oedema, which in primary intrinsic tumour may contain infiltrating angiogenic tumour cells in addition to vasogenic oedema, and in metastatic disease is more likely to reflect pure vasogenic oedema.

Diffusion-weighted imaging and tractography

Diffusion-weighted imaging (DWI) allows quantification of the movement of free water molecules occurring secondarily to random thermal motion. The apparent diffusion coefficient (ADC) is a measure of the degree of random motion of water molecules due to thermal

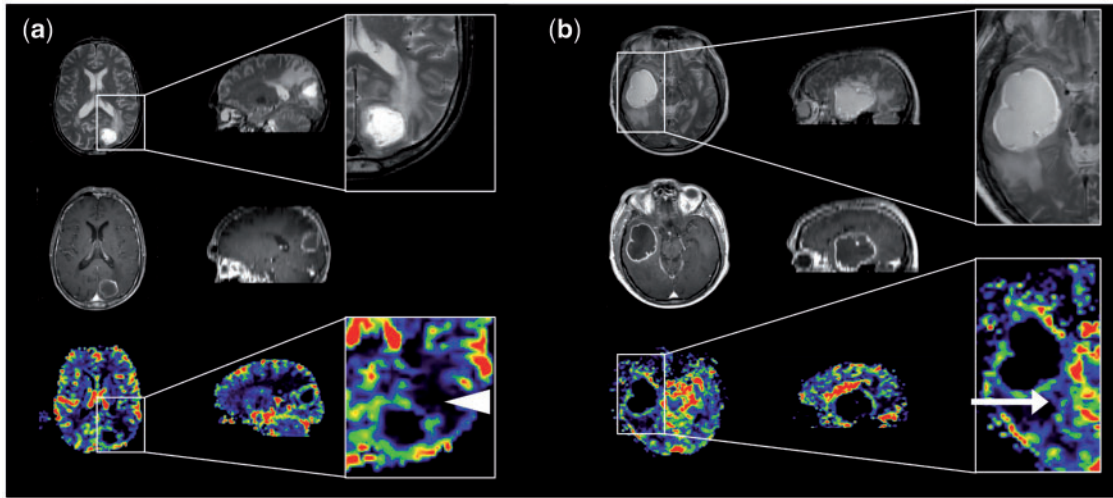


**Figure 3** Perfusion imaging in (a) solitary cerebral metastasis and (b) GBM (axial imaging on the left and sagittal reformats on the right). Top row:  $T_2$ -weighted imaging. Middle row: post-contrast  $T_1$ -weighted imaging. Bottom row: CBV maps. Magnified images of CBV maps and corresponding  $T_2$ -weighted images. (a) The peri-lesional non-enhancing tissue surrounding the metastasis exhibits a very low relative CBV (white arrowhead) and represents vasogenic oedema; (b) the peri-lesional non-enhancing tissue surrounding the GBM has a slightly higher relative cerebral blood volume (white arrow) and represents infiltrating glioma.

energy. The term apparent is used to convey that it is not truly the free diffusion of water that is being observed. On visual inspection of diffusion imaging and ADC maps, there is considerable evidence suggesting that this is of value in distinguishing necrotic tumours (both primary HGGs and metastases) from abscesses, with restricted diffusion seen in the core of abscesses<sup>[34]</sup>. However, it should be noted that the distinction is not clear cut and restricted diffusion has been reported in cerebral metastases of certain histological types (both small and non-small-cell lung, breast, colon and testicular carcinoma) (Fig. 4)<sup>[35]</sup>. The literature regarding the usefulness of measurement of ADC values and related metrics in distinguishing HGG from cerebral metastases is controversial. Some groups have reported higher values of ADC and ADC ratios in the solid tumour<sup>[36,37]</sup> or peritumoural tissue<sup>[36–39]</sup> in cerebral metastases than in HGG, while others have reported lower values in either tumour<sup>[40,41]</sup> or peri-lesional tissue<sup>[42]</sup> and some have reported no significant difference in ADC values between HGG and metastatic disease<sup>[23,43,44]</sup>. These conflicting results may be a reflection of the wide variation in different imaging acquisitions, post-processing analysis techniques and scanners used. In addition, all studies have had relatively small recruitment numbers, few containing more than 20 patients with cerebral metastases and none containing a single metastatic histological tissue type, thus making the data rather heterogeneous and limiting its interpretation and applicability.

The use of diffusion tensor imaging (DTI) allows assessment of different, more detailed, diffusion-based parameters such as mean diffusivity (MD) and fractional anisotropy (FA). MD from DTI takes into account the

orientation of the diffusion ellipsoid in each voxel, while ADC from DWI represents diffusion in the orthogonal measurement directions as applied to every voxel. Confusion can arise from the often interchangeable use of MD and ADC. Like studies evaluating the role of ADC in cerebral metastases, the literature regarding MD and FA measures is also controversial<sup>[38,45,46]</sup>. In a study comparing 16 GBMs with 12 metastases, measures of MD in both tumoural and peri-tumoural tissue was found to be significantly different between metastases and GBM, with low MD values in the solid tumour in metastatic disease ( $0.98 \pm 0.188$ ) compared with GBM ( $1.22 \pm 0.284$ ), and high MD values in the peri-tumoural tissue of metastases ( $1.41 \pm 0.097$ ) versus GBM ( $1.25 \pm 0.201$ ). This study also reported differences in the FA values of the peri-tumoural region, but not the solid tumour between the 2 malignancy types with metastases having significantly lower FA values ( $0.159 \pm 0.02$ ) than GBM ( $0.188 \pm 0.045$ )<sup>[47]</sup>. In comparison, a similar study that included 10 GBMs and 6 metastases reported no significant difference between enhancing tumoural or peri-tumoural tissue MD or FA values, although the MD value of the cystic component was reported to be significantly lower in the metastatic group than the GBM group; however there was considerable overlap between the 2 entities<sup>[48]</sup>. A larger study by Wang et al.<sup>[49]</sup> of 63 patients with ring-enhancing lesions (38 GBMs and 25 metastases) examined more detailed features of the diffusion tensor shape, namely linear and planar coefficients (CL and CP, respectively), in addition to measures of FA and ADC in the tumour core, enhancing rim, immediate peri-tumoural region and distant peri-tumoural region. They reported significantly higher values of both

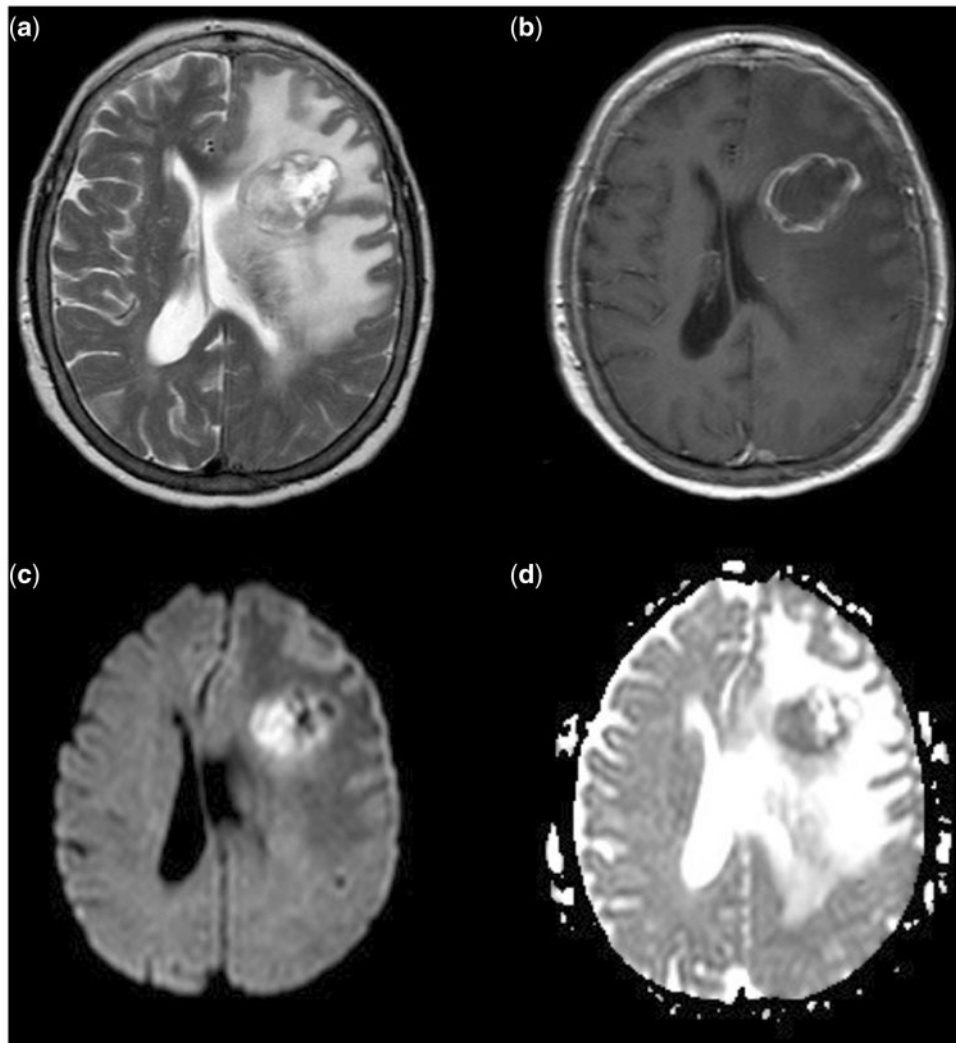


**Figure 4** Restricted diffusion in cerebral metastases. (a)  $T_2$ -weighted imaging; (b) post-contrast  $T_1$ -weighted imaging; (c) DWI; (d) ADC map. There is restricted diffusion within the medial aspect of the tumour which demonstrates restriction in the more solid,  $T_2$  hypointense, non-enhancing component.

FA and CP for all tissue regions and elevated CL in all but the distant peri-tumoural region in GBM tumours compared with cerebral metastases. No significant difference in ADC measures was found between GBM or metastases but the model from this study that best predicted tumour type with a sensitivity of 92% and specificity of 100% included ADC, FA and CP measures. Other scalar measures of directional diffusion that can be derived include  $p$  (pure isotropic diffusion),  $q$  (pure anisotropic diffusion) and  $L$  (the total magnitude of the diffusion tensor). In a comparative study of the value of these measures in distinguishing GBM from metastases, the only parameter found to have a significantly lower value in the cerebral metastases compared with GBM was the measure  $q$  in the peri-tumoural region<sup>[50]</sup>. There is also evidence for the utility of DWI or DTI in discriminating solitary, cystic metastases from cerebral abscesses<sup>[34]</sup>. Since abscesses often exhibit significantly lower central ADC, they can be confused with

mucinous adenocarcinomas. Reiche et al.<sup>[48]</sup> have recently suggested that a combination of central ADC with rim FA helps to distinguish those neoplastic cysts with low central ADC from abscesses.

### Magnetic resonance spectroscopy

Proton magnetic resonance spectroscopy (MRS) allows tissue metabolites to be assessed non-invasively. The 2 main techniques use single voxel (e.g. PRESS, STEAM) or multivoxel chemical shift imaging (CSI) techniques. Details of these approaches can be found in a recent review<sup>[51]</sup>. A number of studies using CSI have shown some potential in differentiating GBM from cerebral metastases, wherein examination of the peri-tumoural region has been reported to show a lower choline (Cho)/creatine (Cr) ratio in cerebral metastases than that seen in GBMs<sup>[32,33,52–55]</sup>. In a study of 53 HGGs and 20 metastases, Server et al.<sup>[54]</sup> reported

100% sensitivity, 88.9% specificity, a positive predictive value (PPV) of 80% and a negative predictive value (NPV) of 100% using a cut-off value of 1.24 for the peri-tumoural Cho/Cr ratio to discriminate between HGG and metastases. Similarly, this group also reported the value of examining the peri-tumoural Cho/NAA ratio and, using a cut-off value of 1.11, found 100% sensitivity, 91.1% specificity, 83.3% PPV, and 100% NPV in discriminating HGG from cerebral metastases. A recent report in 2 cases of mucinous adenocarcinoma has described the presence of a metabolite peak that mimics NAA and may reduce the specificity of MRS in this tumour type<sup>[56]</sup>. The use of short echo time proton spectroscopy allows lipid and macromolecule signals to be observed. These are often found to be high in necrotic tumours. Opstad et al.<sup>[57]</sup> studied the value of short echo time MRS in comparing lipid and macromolecule signals in cerebral metastases ( $n=34$ ) and GBM ( $n=25$ ) and reported significantly higher values in metastases than GBM, although there was considerable overlap between the 2 groups. In an attempt to address the multicenter applicability of single voxel spectroscopy for assisting differential diagnosis of brain tumours, García-Gómez et al.<sup>[58]</sup> assessed spectra from several sites in over 300 intracranial lesions with histological diagnosis. They reported around 90% accuracy in pairwise discriminant analysis for differentiation between meningiomas, low-grade gliomas, GBM and metastases. Unfortunately, the discrimination of GBM from metastasis was less accurate at 78%, and they recommend a combined approach in further work.

The value of MRS in non-invasive discrimination of source tissue in cerebral metastases has been studied by 2 groups<sup>[59,60]</sup>. Chernov et al.<sup>[59]</sup> reported increased mobile lipid content and elevated Lip/nCr in cerebral metastases arising from a colorectal primary when compared with metastases from histologically distinct primary tumours. In addition, Huang et al.<sup>[60]</sup> compared non-small-cell lung carcinoma (NSCLC) cerebral metastases ( $n=40$ ) with those from breast ( $n=17$ ) and melanoma ( $n=9$ ) using CSI MRS, reporting the Cho/Cr ratio to be significantly lower in NSCLC metastases than in either breast or melanoma metastases. MRS can be performed *ex vivo* on biopsy samples for metabolic classification of tumours, and there is evidence for clinically useful differential characterization of cerebral metastases<sup>[61]</sup>. While this is invasive, it provides evidence for the potential use of new metabolic and spectroscopic imaging techniques *in vivo*.

### Multi-parametric imaging

As with many advanced MRI techniques, where optimization of acquisition and analysis requires further work, there is often diagnostic overlap within a particular imaging parameter. Evidence suggests that the ability to distinguish primary HGGs from solitary cerebral metastases

is improved when a multi-parametric imaging approach is taken<sup>[33,53,62]</sup>. Law et al.<sup>[33]</sup> reported significant differences in both rCBV and Cho/Cr in the peri-tumoural region of GBM and metastases and advocated that these imaging parameters could be used together to try and distinguish between the 2 tumour types. Similarly, Bulakbasi et al.<sup>[62]</sup> found both ADC values and MRS values were separately useful in differentiating cerebral tumours, but when combined there was added value in predicting tumour type. The combined use of perfusion-weighted imaging (PWI) and MRS has also shown value in differentiating cerebral metastases originating from primary lung carcinoma from lesions originating from either breast carcinoma or melanoma<sup>[60]</sup>. Wang et al.<sup>[63]</sup> used a combination of DTI and DSC to distinguish GBM, solitary metastases and primary cerebral lymphoma (PCL). They concluded that the best discriminative combination for distinguishing GBM from the other tumour types involved FA from the enhancing rim and rCBV from the peri-tumoural region. This finding is in keeping with the histopathological findings in GBM with pseudopalliating cellular rim, and angiogenesis occurring adjacent to microinvasive disease in the surrounding oedema. Again, the multiparametric approach has been used for the discrimination of infectious from cystic neoplastic lesions. In a relatively small study, the lower central ADC was again found in infectious lesions, while the presence of amino acids on MRS was also indicative of infection<sup>[36]</sup>. In addition, the blood volume in the rim of the neoplastic lesions was found to be higher.

### Conclusions

The evidence regarding the use of advanced imaging techniques in cerebral metastatic disease is largely controversial with a variety of conflicting results regarding the different advanced imaging modalities. The majority of studies have focused on discriminating HGG from solitary cerebral metastases, with fewer studies attempting to differentiate metastatic lesions according to histological subtype, and therefore inform further imaging. At best, the majority of evidence suggests that quantitative metrics derived from PWI, DWI, DTI or MRS of the peri-tumoural tissue may provide a supplementary means of discriminating HGG from cerebral metastases, and the use of a multimodality approach combining parameters derived from each of the advanced imaging techniques is likely to improve both the diagnostic sensitivity and specificity. Unfortunately, most of the current studies are limited with regard to their small patient numbers (few have more than 30 patients for a given tumour type) and the heterogeneous collection of histological types of cerebral metastases that are frequently grouped together. A large multi-centre trial is required to evaluate the usefulness of these combined advanced MR parameters in discriminating both GBM from cerebral metastases, and metastases of different histological subtype. In order to

achieve diagnostic currency in the setting of busy clinical scanners, a selection of optimized advanced MR techniques requiring limited post-processing is desirable. A combination of short echo time MRS, DTI and DSC imaging is a likely combination, with attention paid to both the enhancing tumour itself and the peri-tumoural tissue. The limitations in the receiver operating characteristics of these approaches mean that the expert input of a suitably experienced radiologist with a complete clinical picture will still be crucial in each case.

## References

- [1] Gavrilovic IT, Posner JB. Brain metastases: epidemiology and pathophysiology. *J Neurooncol* 2005; 75: 5–14. doi:10.1007/s11060-004-8093-6.
- [2] Pentheroudakis G, Gofinopoulos V, Pavlidis N. Switching benchmarks in cancer of unknown primary: from autopsy to microarray. *Eur J Cancer* 2007; 43: 2026–36. doi:10.1016/j.ejca.2007.06.023.
- [3] Posner JB, Chernik NL. Intracranial metastases from systemic cancer. *Adv Neurol* 1978; 19: 579–92.
- [4] Bendell JC, Domchek SM, Burstein HJ, et al. Central nervous system metastases in women who receive trastuzumab-based therapy for metastatic breast carcinoma. *Cancer* 2003; 97: 2972–7. doi:10.1002/cncr.11436.
- [5] Dhote R, Beuzeboc P, Thiounn N, et al. High incidence of brain metastases in patients treated with an M-VAC regimen for advanced bladder cancer. *Eur Urol* 1998; 33: 392–5. doi:10.1159/000019622.
- [6] Sperduto PW, Chao ST, Sneed PK, et al. Diagnosis-specific prognostic factors, indexes, and treatment outcomes for patients with newly diagnosed brain metastases: a multi-institutional analysis of 4,259 patients. *Int J Radiat Oncol Biol Phys* 2010; 77: 655–61. doi:10.1016/j.ijrobp.2009.08.025.
- [7] Al-Shamy G, Sawaya R. Management of brain metastases: the indispensable role of surgery. *J Neurooncol* 2009; 92: 275–82. doi:10.1007/s11060-009-9839-y.
- [8] Jenkinson MD, Haylock B, Shenoy A, Husband D, Javadpour M. Management of cerebral metastasis: evidence-based approach for surgery, stereotactic radiosurgery and radiotherapy. *Eur J Cancer* 2011; 47: 649–55. doi:10.1016/j.ejca.2010.11.033.
- [9] Linskey ME, Andrews DW, Asher AL, et al. The role of stereotactic radiosurgery in the management of patients with newly diagnosed brain metastases: a systematic review and evidence-based clinical practice guideline. *J Neurooncol* 2010; 96: 45–68. doi:10.1007/s11060-009-0073-4.
- [10] Brekenfeld C, Foert E, Hundt W, Kenn W, Lodeann KP, Gehl HB. Enhancement of cerebral diseases: how much contrast agent is enough? Comparison of 0.1, 0.2, and 0.3 mmol/kg gadoteridol at 0.2 T with 0.1 mmol/kg gadoteridol at 1.5 T. *Invest Radiol* 2001; 36: 266–75. doi:10.1097/00004424-200105000-00004.
- [11] Kim ES, Chang JH, Choi HS, Kim J, Lee SK. Diagnostic yield of double-dose gadobutrol in the detection of brain metastasis: intraindividual comparison with double-dose gadopentetate dimeglumine. *AJNR Am J Neuroradiol* 2010; 31: 1055–8. doi:10.3174/ajnr.A2010.
- [12] Tomura N, Narita K, Takahashi S, et al. Contrast-enhanced multi-shot echo-planar FLAIR in the depiction of metastatic tumors of the brain: comparison with contrast-enhanced spin-echo T1-weighted imaging. *Acta Radiol* 2007; 48: 1032–7. doi:10.1080/02841850701499425.
- [13] Qian YF, Foert E, Hundt W, Kenn W, Lodeann KP, Gehl HB. MR T1-weighted inversion recovery imaging in detecting brain metastases: could it replace T1-weighted spin-echo imaging? *AJNR Am J Neuroradiol* 2008; 29: 701–4. doi:10.3174/ajnr.A0907.
- [14] Stuckey SL, Wijedeera R. Multicentric/multifocal cerebral lesions: can fluid-attenuated inversion recovery aid the differentiation between glioma and metastases? *J Med Imaging Radiat Oncol* 2008; 52: 134–9. doi:10.1111/j.1440-1673.2008.01931.x.
- [15] Winking M, Wildforster U. Computer tomographic assessment of perifocal edema surrounding tumors of the cerebral cortex. *Neurosurg Rev* 1989; 12: 55–8. doi:10.1007/BF01787130.
- [16] Hakyemez B, Erdogan C, Gokalp G, Dusak A, Parlak M. Solitary metastases and high-grade gliomas: radiological differentiation by morphometric analysis and perfusion-weighted MRI. *Clin Radiol* 2010; 65: 15–20. doi:10.1016/j.crad.2009.09.005.
- [17] Jackson A, O'Connor J, Thompson G, Mills S. Magnetic resonance perfusion imaging in neuro-oncology. *Cancer Imaging* 2008; 8: 186–99. doi:10.1102/1470-7330.2008.0019.
- [18] Thompson G, Mills SJ, Stivaros SM, Jackson AI. Imaging of brain tumors: perfusion/permeability. *Neuroimaging Clin N Am* 2010; 20: 337–53. doi:10.1016/j.nic.2010.04.008.
- [19] Lacerda S, Law M. Magnetic resonance perfusion and permeability imaging in brain tumors. *Neuroimaging Clin North Am* 2009; 19: 527–57. doi:10.1016/j.nic.2009.08.007.
- [20] Jackson A. Analysis of dynamic contrast enhanced MRI. *Br J Radiol* 2004; 77(Spec No. 2): S154–66. doi:10.1259/bjr/16652509.
- [21] Ludemann L, Grieger W, Wurm R, Wust P, Zimmer C. Quantitative measurement of leakage volume and permeability in gliomas, meningiomas and brain metastases with dynamic contrast-enhanced MRI. *Magn Reson Imaging* 2005; 23: 833–41. doi:10.1016/j.mri.2005.06.007.
- [22] Young GS, Setayesh K. Spin-echo echo-planar perfusion MR imaging in the differential diagnosis of solitary enhancing brain lesions: distinguishing solitary metastases from primary glioma. *AJNR Am J Neuroradiol* 2009; 30: 575–7. doi:10.3174/ajnr.A1239.
- [23] Calli C, Kitis O, Yuntun N, Yurtseven T, Islekel S, Akalin T. Perfusion and diffusion MR imaging in enhancing malignant cerebral tumors. *Eur J Radiol* 2006; 58: 394–403. doi:10.1016/j.ejrad.2005.12.032.
- [24] Erdogan C, Hakyemez B, Yildirim N, Parlak M. Brain abscess and cystic brain tumor: discrimination with dynamic susceptibility contrast perfusion-weighted MRI. *J Comput Assist Tomogr* 2005; 29: 663–7. doi:10.1097/01.rct.0000168868.50256.55.
- [25] Muccio CF, Esposito G, Bartolini A, Cerase A. Cerebral abscesses and necrotic cerebral tumours: differential diagnosis by perfusion-weighted magnetic resonance imaging. *Radiol Med* 2008; 113: 747–57. doi:10.1007/s11547-008-0254-9.
- [26] Chan JH, Tsui EY, Chau LF, et al. Discrimination of an infected brain tumor from a cerebral abscess by combined MR perfusion and diffusion imaging. *Comput Med Imaging Graph* 2002; 26: 19–23. doi:10.1016/S0895-6111(01)00023-4.
- [27] Hakyemez B, Erdogan C, Bolca N, Yildirim N, Gokalp G, Parlak M. Evaluation of different cerebral mass lesions by perfusion-weighted MR imaging. *J Magn Reson Imaging* 2006; 24: 817–24. doi:10.1002/jmri.20707.
- [28] Hakyemez B, Yildirim N, Erdoğan C, Kocaeli H, Korfali E, Parlak M. Meningiomas with conventional MRI findings resembling intraaxial tumors: can perfusion-weighted MRI be helpful in differentiation? *Neuroradiology* 2006; 48: 695–702. doi:10.1007/s00234-006-0115-y.
- [29] Fayed N, Modrego PJ. The contribution of magnetic resonance spectroscopy and echoplanar perfusion-weighted MRI in the initial assessment of brain tumours. *J Neurooncol* 2005; 72: 261–5. doi:10.1007/s11060-004-2180-6.
- [30] Bulakbasi N, Kocaoglu M, Farzaliyev A, Tayfun C, Ucoz T, Somuncu I. Assessment of diagnostic accuracy of perfusion MR imaging in primary and metastatic solitary malignant brain tumors. *AJNR Am J Neuroradiol* 2005; 26: 2187–99.
- [31] Rollin N, Guyotat J, Streichenberger N, Honnorat J, Tran Minh VA, Cotton F. Clinical relevance of diffusion and

- perfusion magnetic resonance imaging in assessing intra-axial brain tumors. *Neuroradiology* 2006; 48: 150–9. doi:10.1007/s00234-005-0030-7.
- [32] Chiang IC, Kuo YT, Lu CY, et al. Distinction between high-grade gliomas and solitary metastases using peritumoral 3-T magnetic resonance spectroscopy, diffusion, and perfusion imagings. *Neuroradiology* 2004; 46: 619–27.
- [33] Law M, Cha S, Knopp EA, Johnson G, Arnett J, Litt AW. High-grade gliomas and solitary metastases: differentiation by using perfusion and proton spectroscopic MR imaging. *Radiology* 2002; 222: 715–21. doi:10.1148/radiol.2223010558.
- [34] Kim YJ, Chang KH, Song IC, et al. Brain abscess and necrotic or cystic brain tumor: discrimination with signal intensity on diffusion-weighted MR imaging. *AJR Am J Roentgenol* 1998; 171: 1487–90.
- [35] Duygulu G, Ovali GY, Calli C, et al. Intracerebral metastasis showing restricted diffusion: correlation with histopathologic findings. *Eur J Radiol* 2010; 74: 117–20. doi:10.1016/j.ejrad.2009.03.004.
- [36] Chiang IC, Hsieh TJ, Chiu ML, Liu GC, Kuo YT, Lin WC. Distinction between pyogenic brain abscess and necrotic brain tumour using 3-tesla MR spectroscopy, diffusion and perfusion imaging. *Br J Radiol* 2009; 82: 813–20. doi:10.1259/bjr/90100265.
- [37] Krabbe K, Gideon P, Wagn P, Hansen U, Thomsen C, Madsen F. MR diffusion imaging of human intracranial tumours. *Neuroradiology* 1997; 39: 483–9. doi:10.1007/s002340050450.
- [38] Lu S, Ahn D, Johnson G, Cha S. Peritumoral diffusion tensor imaging of high-grade gliomas and metastatic brain tumors. *AJNR Am J Neuroradiol* 2003; 24: 937–41.
- [39] Pavlisa G, Rados M, Pavlisa G, Pavic L, Potocki K, Mayer D. The differences of water diffusion between brain tissue infiltrated by tumor and peritumoral vasogenic edema. *Clin Imaging* 2009; 33: 96–101. doi:10.1016/j.clinimag.2008.06.035.
- [40] Bulakbasi N, Guvenc I, Onguru O, Erdogan E, Tayfun C, Ucoz T. The added value of the apparent diffusion coefficient calculation to magnetic resonance imaging in the differentiation and grading of malignant brain tumors. *J Comput Assist Tomogr* 2004; 28: 735–46. doi:10.1097/00004728-200411000-00003.
- [41] Server A, Kulle B, Maehlen J, et al. Quantitative apparent diffusion coefficients in the characterization of brain tumors and associated peritumoral edema. *Acta Radiol* 2009; 50: 682–9. doi:10.1080/02841850902933123.
- [42] Lee EJ, terBrugge K, Mikulis D, et al. Diagnostic value of peritumoral minimum apparent diffusion coefficient for differentiation of glioblastoma multiforme from solitary metastatic lesions. *AJR Am J Roentgenol* 2011; 196: 71–6. doi:10.2214/AJR.10.4752.
- [43] Yamasaki F, Kurisu K, Satoh K, et al. Apparent diffusion coefficient of human brain tumors at MR imaging. *Radiology* 2005; 235: 985–91. doi:10.1148/radiol.2353031338.
- [44] Guzman R, Altrichter S, El-Koussy M, et al. Contribution of the apparent diffusion coefficient in perilesional edema for the assessment of brain tumors. *J Neuroradiol* 2008; 35: 224–9.
- [45] Lu S, Ahn D, Johnson G, Law M, Zagzag D, Grossman RI. Diffusion-tensor MR imaging of intracranial neoplasia and associated peritumoral edema: introduction of the tumor infiltration index. *Radiology* 2004; 232: 221–8. doi:10.1148/radiol.2321030653.
- [46] Tsuchiya K, Fujikawa A, Nakajima M, Honya K. Differentiation between solitary brain metastasis and high-grade glioma by diffusion tensor imaging. *Br J Radiol* 2005; 78: 533–7. doi:10.1259/bjr/68749637.
- [47] Byrnes TJ, Barrick TR, Bell BA, Clark CA. Diffusion tensor imaging discriminates between glioblastoma and cerebral metastases in vivo. *NMR Biomed* 2011; 24: 54–60. doi:10.1002/nbm.1555.
- [48] Reiche W, Schuchardt V, Hagen T, Il'yasov KA, Billmann P, Weber J. Differential diagnosis of intracranial ring enhancing cystic mass lesions—role of diffusion-weighted imaging (DWI) and diffusion-tensor imaging (DTI). *Clin Neurol Neurosurg* 2010; 112: 218–25. doi:10.1016/j.clineuro.2009.11.016.
- [49] Wang S, Kim S, Chawla S, et al. Differentiation between glioblastomas and solitary brain metastases using diffusion tensor imaging. *Neuroimage* 2009; 44: 653–60. doi:10.1016/j.neuroimage.2008.09.027.
- [50] Wang W, Steward CE, Desmond PM. Diffusion tensor imaging in glioblastoma multiforme and brain metastases: the role of p, q, L, and fractional anisotropy. *AJNR Am J Neuroradiol* 2009; 30: 203–8. doi:10.3174/ajnr.A1303.
- [51] van der Graaf M. In vivo magnetic resonance spectroscopy: basic methodology and clinical applications. *Eur Biophys J* 2010; 39: 527–40. doi:10.1007/s00249-009-0517-y.
- [52] Chawla S, Zhang Y, Wang S, et al. Proton magnetic resonance spectroscopy in differentiating glioblastomas from primary cerebral lymphomas and brain metastases. *J Comput Assist Tomogr* 2010; 34: 836–41. doi:10.1097/RCT.0b013e3181ec554e.
- [53] Bendini M, Marton E, Feletti A, et al. Primary and metastatic intraaxial brain tumors: prospective comparison of multivoxel 2D chemical-shift imaging (CSI) proton MR spectroscopy, perfusion MRI, and histopathological findings in a group of 159 patients. *Acta Neurochir (Wien)* 2011; 153: 403–12. doi:10.1007/s00701-010-0833-0.
- [54] Server A, Josefsen R, Kulle B, et al. Proton magnetic resonance spectroscopy in the distinction of high-grade cerebral gliomas from single metastatic brain tumors. *Acta Radiol* 2010; 51: 316–25. doi:10.3109/02841850903482901.
- [55] Fan G, Sun B, Wu Z, Guo Q, Guo Y. In vivo single-voxel proton MR spectroscopy in the differentiation of high-grade gliomas and solitary metastases. *Clin Radiol* 2004; 59: 77–85. doi:10.1016/j.crad.2003.08.006.
- [56] Liu X, Germin BI, Zhong J, Ekholm S. N-Acetyl peak in MR spectra of intracranial metastatic mucinous adenocarcinomas. *Magn Reson Imaging* 2010; 28: 1390–4. doi:10.1016/j.mri.2010.06.015.
- [57] Opstad KS, Murphy MM, Wilkins PR, Bell BA, Griffiths JR, Howe FA. Differentiation of metastases from high-grade gliomas using short echo time 1H spectroscopy. *J Magn Reson Imaging* 2004; 20: 187–92. doi:10.1002/jmri.20093.
- [58] Garcia-Gomez JM, Luts J, Julia-Sapé M, et al. Multiproject-multicenter evaluation of automatic brain tumor classification by magnetic resonance spectroscopy. *Magma* 2009; 22: 5–18. doi:10.1007/s10334-008-0146-y.
- [59] Chernov MF, Ono Y, Kubo O, Hori T. Comparison of 1H-MRS-detected metabolic characteristics in single metastatic brain tumors of different origin. *Brain Tumor Pathol* 2006; 23: 35–40. doi:10.1007/s10014-006-0198-5.
- [60] Huang BY, Kwock L, Castillo M, Smith JK. Association of choline levels and tumor perfusion in brain metastases assessed with proton MR spectroscopy and dynamic susceptibility contrast-enhanced perfusion weighted MRI. *Technol Cancer Res Treat* 2010; 9: 327–37.
- [61] Sjobakk TE, Johansen R, Bathen TF, et al. Characterization of brain metastases using high-resolution magic angle spinning MRS. *NMR Biomed* 2008; 21: 175–85. doi:10.1002/nbm.1180.
- [62] Bulakbasi N, Kocaoglu M, Örsa F, Tayfun C, Üçöz T. Combination of single-voxel proton MR spectroscopy and apparent diffusion coefficient calculation in the evaluation of common brain tumors. *AJNR Am J Neuroradiol* 2003; 24: 225–33.
- [63] Wang S, Kim S, Chawla S, et al. Differentiation between glioblastomas, solitary brain metastases, and primary cerebral lymphomas using diffusion tensor and dynamic susceptibility contrast-enhanced MR imaging. *AJNR Am J Neuroradiol* 2011; 32: 507–14. doi:10.3174/ajnr.A2333.